International Journal of Thermophysics, Vol. 25, No. 6, November 2004 (© 2004)

Surface Tension Measurements on CMSX-4 Superalloy by the Drop-Weight and Oscillating-Drop Methods

B. Vinet,[1,2] S. Schneider,[3] J. P. Garandet,[1] B. Marie,[1] B. Drevet,[1] and I. Egry[3]

Received December 10, 2003

The surface tension of the CMSX-4® superalloy has been determined by the drop-weight and oscillating-drop methods which are well adapted to reactive materials. The recommended values are $1.59\,\mathrm{J{\cdot}m^{-2}}$ for the surface tension at the liquidus temperature and $-0.14\times10^{-3}\,\mathrm{J{\cdot}m^{-2}{\cdot}K^{-1}}$ for the temperature coefficient. A conclusion of the present work is that the interpretation of surface tension measurements performed on a complex alloy generally requires additional work to be performed on simpler associated binary or ternary systems, as well as some support from solidification experiments.

KEY WORDS: CMSX-4® superalloy; drop-weight method; electromagnetic levitation; Ni–Al system; oscillating-drop technique; surface tension.

1. INTRODUCTION

The surface tension (σ) of liquid metals is of both technical and scientific importance. It can be related to casting and welding processes and is also relevant for wetting phenomena [1]. Among the different techniques developed for surface-tension measurements [2], the oscillating-drop technique has received great attention as this containerless technique offers the possibility to carry out surface-tension measurements for both the stable and metastable liquid states, and alternatively under earth or microgravity conditions [3]. In comparison with other methods, it has a wide range of accessible temperatures, including low melting point as well as

[1]Commissariat à l'Énergie Atomique, Département des Technologies pour les Énergies Nouvelles, 17 rue des Martyrs, 38054 Grenoble Cedex 09, France.
[2]To whom correspondence should be addressed. E-mail: vinet@chartreuse.cea.fr
[3]Institut für Raumsimulation, DLR, Linder Höhe, D-51170 Köln, Germany.

0195-928X/04/1100-1889/0

refractory metals. In order to eliminate potential systematic errors inherent in this technique, it is of key importance to carry out measurements with alternative methods, whenever possible. In particular, there is some interest to compare experiments performed with the drop-weight method. Indeed, the drop-weight method offers the advantage to provide reference data of the surface tension at the melting (or liquidus) temperature, while the oscillating-drop technique, when carried out on earth, is based on a complex mathematical treatment due to asymmetric droplets and processing conditions. However, only the oscillating-drop technique can provide measurements of temperature coefficients of surface tension in the high-temperature field. More generally, containerless processing by electromagnetic [4], electrostatic [5], or aerodynamic [6] levitations should assume a growing importance for both development (new compositions) and thermophysical property measurements (σ, density, viscosity, etc.) of advanced high-temperature metallic materials (e.g., Nb-based alloys, Pt-based superalloy, etc. [7]).

This work, performed within the ESA-funded Thermolab project, focuses on the CMSX-4® superalloy. The oscillating-drop technique has been applied using the electromagnetic levitation facility available at DLR [4, 8]. The pendant-drop configuration has been implemented at the top of the 48-m high Grenoble drop-tube in the course of nucleation studies on falling refractory droplets [7]. The operation of this configuration under ultrahigh vacuum conditions has already allowed us to obtain new determinations of the surface tension of several refractory metals [9, 10], as well as to get some insight into the physics of the detachment problem of pendant volumes [11]. More recently, evidence has been gained on the possibility for the drop-weight method to deliver reliable surface-tension measurements for alloys at the liquidus temperature [12]. In this context, the study of the complex CMSX-4® superalloy may appear as a new test for this method which is attractive for its simplicity. The CMSX-4® is a Ni-based superalloy that is a registered trademark of the Cannon-Muskegon Corporation. It has been developed among other single crystal alloys containing Re (e.g., PWA 1484, SC 180, René N5, etc.) for a variety of turbine engine applications [13].

2. EXPERIMENTAL APPROACH BY THE DROP-WEIGHT METHOD

2.1. Drop-Weight Method

The pendant-drop configuration consists of heating the end of a wire of the material, which forms a pendant drop on melting. The droplet

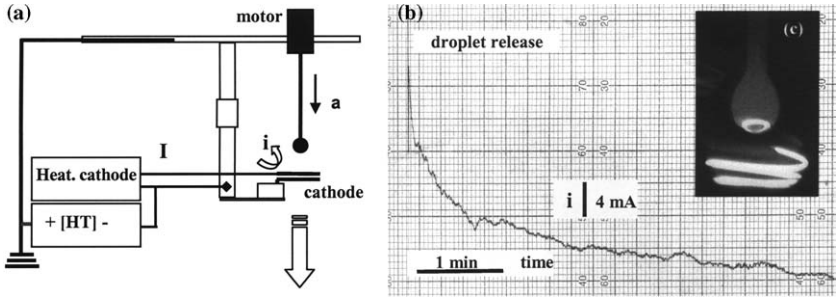

Fig. 1. (a) Schematic for electron bombardment melting. Current I heats the cathode and promotes thermo-electronic emission. Melting is obtained when applying a negative voltage (< 1.5kV). A reduction geared motor, giving motorized speeds ($a \approx 2$ mm min^{-1}), moves the wire downward over a maximum distance of 220 mm; (b) monotonic evolution of the electronic current during elaboration; (c) picture of a CMSX-4 pendant droplet.

growth is driven by a small amount of overheating which has to be compensated by a downward movement of the wire/rod to maintain the pendant volume at the same level (Fig. 1a). The droplet detaches itself from the rod when the surface tension can no longer balance its increasing weight. Through this method, surface-tension (σ) measurements are based on the release conditions written as

$$\sigma = \frac{mg^{\circ}}{2\pi r^{\circ}\alpha F}. \tag{1}$$

where m is the mass of the collected drop, g° is the gravitational acceleration, r° is the radius of the cylindrical wire at room temperature and α is the ratio of the wire diameters between working (melting) and ambient temperatures (Eq. (2a)) . This ratio is derived from densities of the solid at the corresponding temperatures (respectively, $\rho_{\mathrm{sol}}^{\mathrm{m}}$ and $\rho_{\mathrm{sol}}^{\circ}$). F is Harkins' empirical factor [14] which is plotted as a function of $\delta = \alpha r^{\circ}/V^{1/3}$ where V is the volume of the droplet (i.e., the ratio of the droplet mass to the liquid density ρ_{liq} at the melting T_{m} or liquidus T_{liq} temperatures). It was later shown that the physical origin of this factor lies within the hydrostatic effect, which is not included in Eq. (1) [11]. The discrepancy between experimental and theoretical values for F is less than 0.25% for F values around 0.8 (i.e., $2r^{\circ}$ of about 1.5 mm). Since the mass is determined with great accuracy, the ultimate limit for the method is correlated with small fluctuations of the wire diameter. This explains why this method results in a high reproducibility of the surface tension. For alloys, each density ($\rho_{\mathrm{sol}}^{\mathrm{o}}$, $\rho_{\mathrm{sol}}^{\mathrm{m}}$, and ρ_{liq}) is calculated from the values corresponding to the pure elements assuming the additivity of volumes (see Eq. (2b) where x_i is the

mass percentage of element i in the alloy). On the one hand, the volume additivity hypothesis is a convenient simplification, but its validity may be questionable. On the other hand, the drop-weight method offers the advantage to re-calculate the surface tension using a new set of densities, if a more accurate set becomes available.

$$\alpha = \left(\frac{\rho_{\mathrm{Sol}}^{\mathrm{o}}}{\rho_{\mathrm{Sol}}^{\mathrm{m}}} \right)^{1/3} \qquad \rho = \frac{\sum m_i}{\sum v_i} = \frac{100}{\sum x_i / \rho_i} \tag{2a,b}$$

2.2. Apparatus and Procedure

Melting of the rod is realized by electron bombardment heating under ultrahigh vacuum conditions, e.g., $\approx 10^{-6}$ Pa when studying the CMSX-4® superalloy (Fig. 1a) [9]. Nonetheless, as discussed in a recent paper [12], secondary vacuum conditions are enough to guarantee the absence of pollution from the environment which is valuable for a more common implementation of this technique, e.g., for production control. The product of the measured electronic current i and the voltage V is often of the order of the theoretical heat lost by both radiation and conduction along the wire (≈ 1 W in the case of the CMSX-4® superalloy). The efficiency of the electron bombardment heating is thus very high, which translates into a relatively low temperature of the tungsten cathode. A simple comparison of cathode and refractory droplet brightnesses results in an estimate of about 2200 K for the cathode temperature. Consequently, pollution from the cathode can be ignored as the vapour pressure of tungsten (10^{-8} Pa) is then below the vacuum level. A number of issues regarding the experimental conditions (droplet temperature and composition uniformity, wire size) have been examined in our previous paper [12]. The study of the CMSX-4® superalloy leads to additional insights of major practical importance.

Although theoretically there should be no effect of the original rod size on the drop-weight (DW) measurement, this result can only be obtained on strictly gas-free specimens; this point has been systematically verified when larger rods (4–6 mm) were zone melted. Indeed, the effect of entrapped gases (sintered rods) or porosities (cast materials) has been identified to be detrimental for reliable DW measurements manifesting in our case through a large spread δm of droplet masses. Indeed, the thinner the wire, the more efficient is the out-gassing for a given pumping flow. Concerning cast materials, X-ray radiographs have been taken to insure droplet releases in a porosity-free zone of the rods. As for other techniques dealing with droplets, the choice of the diameter rod/wire could be of practical importance. The diameter of larger drops tends to equal that

of the support allowing little control of power parameters, as melting and droplet release are almost simultaneous. Moreover, such a large size does not favor a flat and horizontal liquid–solid interface. On the other hand, the use of the thinnest wires (< 0.5 mm) was not straightforward either, as one needs to continuously adjust the parameters during the experiment, which can be detrimental to the droplet stability. To sum things up, our experience is that the optimal wire diameter should be taken between 1 and 3 mm. However, in the case of alloys which are not commonly supplied in the form of wires, it may be difficult to provide well-defined cylindrical samples, as was the case in the CMSX-4® study.

The first rods used (designated as R1 and R2) were far from cylindrical with significant fluctuations of the diameter along the length ($\pm 3\%$). Encouragingly enough, very stable pendant droplets were obtained during the two experiment runs performed on these rods. In particular, the evolution of the electric current, which is usually a good indicator of the quality for both the droplet growth and the droplet release, did not show jolts or peaks until release (Fig. 1b). Nonetheless, a new procedure has been adopted for the second set of rods (designated as R3 and R4) by defining accurately their profiles. The diameter has been measured every ≈ 2.4mm along the length of each rod. The diameter was determined as an average value between two measurements realized at 90° from each other. After the experiments were completed, these profiles were used to determine the local diameter where droplet release happened, simply by converting the mass of the collected droplet to a length (Fig. 2). The mass lost by evaporation is negligible, as the time for elaboration is only a few minutes. Moreover, these two rods R3 and R4 have been mechanically cleaned by scratching using a knife before implementation in the melting furnace. The mass lost during scratching being 0.15% of the rod mass, this preparation has a negligible effect on the nominal diameter ($\Delta d/d = 1/2\Delta m/m$).

When applied to alloys, there could be an uncertainty in the temperature determination due to the existence of a solidification interval. Nonetheless, nucleation studies performed in the Grenoble drop tube have given great confidence in the fact that the initial temperature corresponds to the liquidus temperature with a small overheating. The high reproducibility of this temperature is due to the slow melting of the wire/rod characterized by a solid-liquid interface of very small size. Keeping in mind that a fresh solid–liquid interface is continuously obtained, this configuration obviously favors chemical homogenization. An insight into this aspect can be derived though an inspection of the dropping tip. Indeed, a small liquid mass adjacent to the rod remains stuck after release and only the liquid fraction hanging below the minimum cross section (neck) is detached.

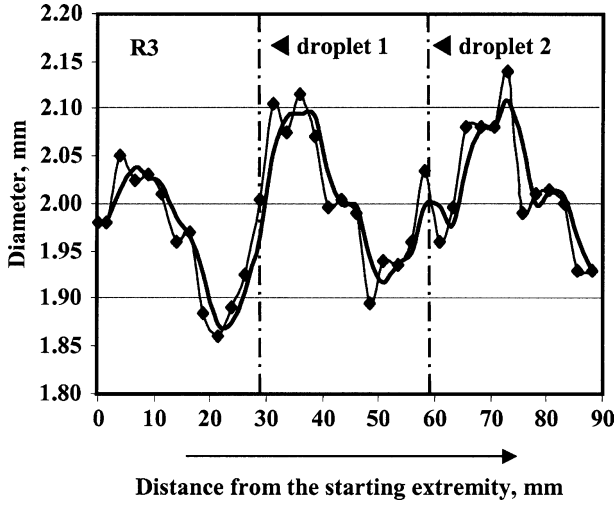

Fig. 2. Measurements of the mean diameter for the rod R3 (−♦−) at different positions along its length. The black line corresponds to a 'sliding average curve of period 2'. The vertical line identifies the zone of the rod where each droplet release occurred.

This phenomenon is taken into account through Harkin's correction factor, keeping in mind that F cannot be simply identified with the ratio of the liquid mass sticking to the wire to the detached volume [11]. A cut of the dropping tip reveals a well-defined solid/liquid interface. Finally, the measurement of essentially the same surface tension for all five collected droplets (see Section 4) demonstrates the reproducibility of the experimental conditions.

3. EXPERIMENTAL APPROACH BY THE OSCILLATING-DROP TECHNIQUE

3.1. Oscillating-Drop Technique

With the oscillating-drop method, the frequency of surface oscillations of the sample around the equilibrium shape is measured. According to Rayleigh [15] the relation between the surface tension σ of a nonrotating spherical sample and the oscillation frequency ω_R (called the Rayleigh frequency in the following) is given by the Rayleigh law:

$$\omega_R^2(\ell) = \ell(\ell-1)(\ell+2)\frac{4\pi}{3}\frac{\sigma}{m} \tag{3}$$

where ℓ is an integer, which depends on the oscillation mode (see Eq. (4)). The mass m of the droplet is determined by weighing or can be calculated via the liquid density. The shape of the oscillating sample can be described by associated Legendre functions:

$$R_l^k(\vartheta, \varphi, t) = a_0 + a_l^k(t) P_l^k(\vartheta) \cos(k\varphi) \tag{4}$$

where θ and ϕ are polar coordinates, t is time, and l and k are integer indices. In electromagnetic levitation, the lowest observed oscillation mode belongs to $\ell = 2$. Oscillation modes with $\ell > 2$ are not observed, because of their strong damping. For an undisturbed oscillating spherical droplet, the frequency does not depend on k.

For the necessary contactless handling of the droplet, we use electromagnetic levitation. Here the metal sample is placed in an alternating magnetic field, which induces eddy currents in the material. Interacting with the field, these currents generate a Lorentz force which supports the sample against gravity. Furthermore, the currents also heat and melt the sample. However, as a result of the magnetic force, aspherical equilibrium shape [16], and rotation of the sample [17], the single Rayleigh frequency for the different surface oscillation modes of the ideal spherical sample splits into five unequally spaced peaks. The degeneracy of the oscillation frequency is cancelled and the oscillation frequencies for $k = -2, -1, 0, 1, 2$ are distinguishable. In particular, the magnetic force effect has been calculated in Ref. [16]. The Rayleigh frequency for = 2 can be obtained from these shifted oscillation frequencies $\omega_{2,k}$:

$$\omega_{2,0}^2(2) = \omega_{\mathrm{R}}^2 + \omega_t^2 \left(3.832 - 0.1714 \frac{z_0^2}{R}\right) \tag{5}$$

$$\omega_{2,1}^2(2) = \omega_{\mathrm{R}}^2 + \omega_t^2 \left(3.775 + 0.5143 \frac{z_0^2}{R}\right) \tag{6}$$

$$\omega_{2,2}^2(2) = \omega_{\mathrm{R}}^2 + \omega_t^2 \left(-0.9297 + 2.571 \frac{z_0^2}{R}\right) \tag{7}$$

$$\text{with} \quad z_0 = \frac{g^\circ}{2\omega_t^2}, \tag{8}$$

where ω_t^2 denotes the mean translation frequency of the sample and g° is the gravitational acceleration. Processing of the data with digital image processing enables the association of the oscillation modes to the

corresponding oscillation frequencies [18]. These oscillation frequencies $\omega_{2,k}$ and ω_t are the input data for the above formulae. The Rayleigh frequency can be calculated from the above equations, and the surface tension via Eq. (3).

3.2. Apparatus and Procedure

The electromagnetic levitation facility consists of a small vacuum chamber and an optical system. The levitation coil is powered by a 24 kW Huettinger HF generator operating at 300–500 kHz. The temperature, which is controlled by convective gas cooling, is measured with a single-color infrared pyrometer covering a temperature range from 550 to 2000°C. In this study, the pyrometer is adjusted to the liquidus temperature of CMSX-4®, i.e., 1380°C. Three types of cooling gases (purity 99.999%) were used for CMSX-4® samples, namely, pure helium, argon, and a mixture of helium and hydrogen (8% hydrogen). Several samples of approximately 1 g have been cut to a cubic form from the supplied rod and levitated. It turned out that samples processed under an argon atmosphere developed a hard crust within a few minutes which suppressed all surface oscillations. This crust is an oxide layer, as has been confirmed by energy dispersive X-ray (EDX) analysis.

The surface oscillations of the liquid droplet were recorded with a digital camera with a frame rate of 125 Hz, and for each selected temperature, 8192 images have been acquired. The images were taken from the top, i.e., along the symmetry axis of the drop. For this viewing direction, the $k=0$ and $k=\pm 2$ modes can be easily identified by taking the sum and difference of two perpendicular radii. From Eq. (4) we have

$$S^{-}(2,0) = R_2^0(\vartheta,\varphi,t) - R_2^0(\vartheta,\varphi+\pi/2,t) = 0 \tag{9}$$

$$\text{and} \quad S^{+}(2,\pm 2) = R_2^{\pm 2}(\vartheta,\varphi,t) + R_2^{\pm 2}(\vartheta,\varphi+\pi/2,t) = \text{const} \tag{10}$$

Consequently, the $k=0$ mode is missing in the frequency spectrum of the radius sum, whereas $k=\pm 2$ is not present in the Fourier transform of the difference signal. This is shown schematically in Fig. 3. Therefore, two perpendicular radii of the sample's image as well as its area and the coordinates of its mass center were derived for each frame. A subsequent fast Fourier transformation (FFT) yields the frequencies of the surface oscillations and sample translations. From the FFT of the sum and difference of the two perpendicular radii, the oscillations peaks in the spectra can be related to the corresponding oscillation modes (Fig. 4).

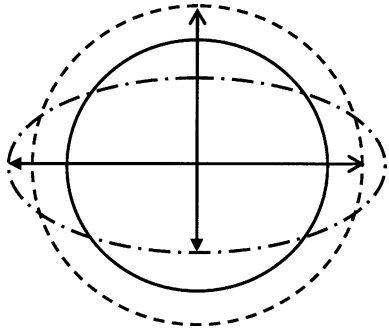

Fig. 3. Oscillation amplitudes in the $k = 0$ (dotted line) and $k = 2$ (dashed line) modes around the equilibrium shape (full circle). For $k = 0$, the difference of two perpendicular radii (upper and right arrow) is time independent, whereas for $k = 2$ the sum (left and bottom arrow) remains constant.

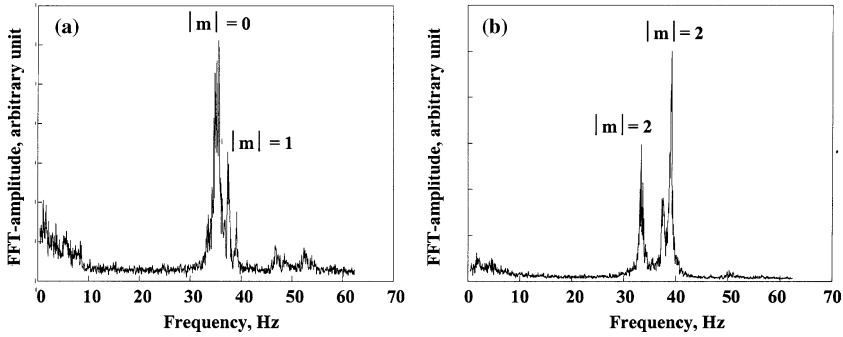

Fig. 4. (a) Frequency spectrum of the radius sum for CMSX-4: the $k = \pm 2$ peak is suppressed; (b) frequency spectrum of the radius difference for CMSX-4, the $k = 0$ peak is suppressed.

4. RESULTS

From the properties of the pure elements, we have assumed a liquid density of $7.79\,\mathrm{g\cdot cm^{-3}}$ and a coefficient α of 1.027 (Eq. (2)). In the course of the first drop-weight set of experiments (R1 and R2), the main diameter has been derived from numerous measurements randomly carried out along the lengths of the rods. Even though the two measurements displayed the same value of $1.58\,\mathrm{J\cdot m^{-2}}$, this agreement should be considered as fortuitous considering the large scatter on rod diameters ($\pm 3\%$).

In this context, a better determination of the local diameter when droplet release happens has been realized for the second set of measurements. In practice, we have taken into account for R3 (leading to the elaboration of two droplets) and R4 a mean value between the diameters derived from the broken curve that links the measurements and the 'sliding average curve of period 2' (bold curve in Fig. 2). The derived surface tensions are 1.58, 1.59, and 1.61 $J \cdot m^{-2}$. On the one hand, the spread of measurements is slightly larger ($\pm 1.3\%$) than was proposed for a truly relevant 'recommended value' at the liquidus temperature. On the other hand, the scatter could be significantly reduced only for rods of well-controlled geometry. Nonetheless, the reproducibility of measurements remains remarkable, considering the poor geometrical quality of the supplied rods. A few scattered oxide particles are observed on the surface of the dropping tip (Fig. 5a), but not on the received droplet (Fig. 5b), as confirmed from X-ray analysis.

The surface tension of CMSX-4® has been measured by the oscillating-drop technique over a temperature range of 250°C around the melting point and for undercoolings up to 75°C (Fig. 6). The liquidus temperature of 1380°C has been determined in the course of the Thermolab project [19]. The straight line shows a linear least-squares fit to the measurement values which have been obtained with helium or helium–hydrogen gas atmosphere around the sample. The values which have been obtained under an argon gas atmosphere have not been used due to the surface contamination of the samples with oxygen. The fit leads to the following equation (in $J \cdot m^{-2}$):

$$\sigma = 1.54 - 0.14 \times 10^{-3} J \cdot m^{-2} (T - 1380°C) \tag{11}$$

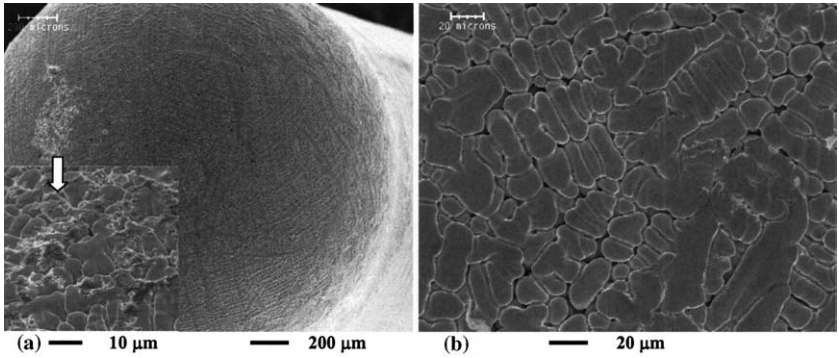

Fig. 5. (a) Bottom view of the dropping tip showing scarce oxide particles; (b) surface aspect of the collected droplet (SEM observations).

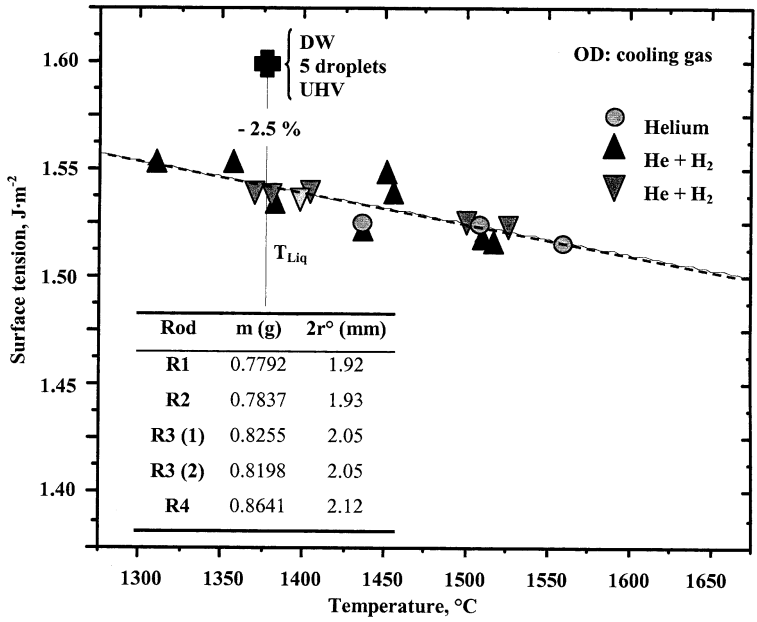

Fig. 6. Surface tension measurements by both DW and OD methods: symbols indicate the type of the cooling gas that has been used to control the temperature of the sample.

The magnetic field effect was taken into account by applying Eqs. (5–7), compensating the apparent rise in surface tension as mentioned in Ref. [20]. The pyrometric temperature measurement is influenced by two effects. These are the error in the determination of the liquidus temperature and the unknown temperature dependence of the emissivity. The former is, however, the dominant source of error. We estimate that the combined error of both effects is $\pm 10°C$ over the entire temperature range. The error in the surface-tension data is due to the error in mass determination and frequency measurement. We estimate $\Delta m = 0.1\%$ and $\Delta\omega = 1\%$, leading to $\Delta\sigma = 2\%$ ($\pm 0.03\,\mathrm{J\cdot m^{-2}}$). Consequently, the differences in surface-tension measurements at the liquidus temperature by the drop-weight and oscillating-drop methods are within the experimental uncertainties. Both experimental results, obtained by the drop-weight method and the oscillating-drop technique, are shown in Fig. 6.

5. DISCUSSION

Without disclosing proprietary information, it can be stated that a standard CMSX-4® superalloy contains typically (in at%) Ni (64.0),

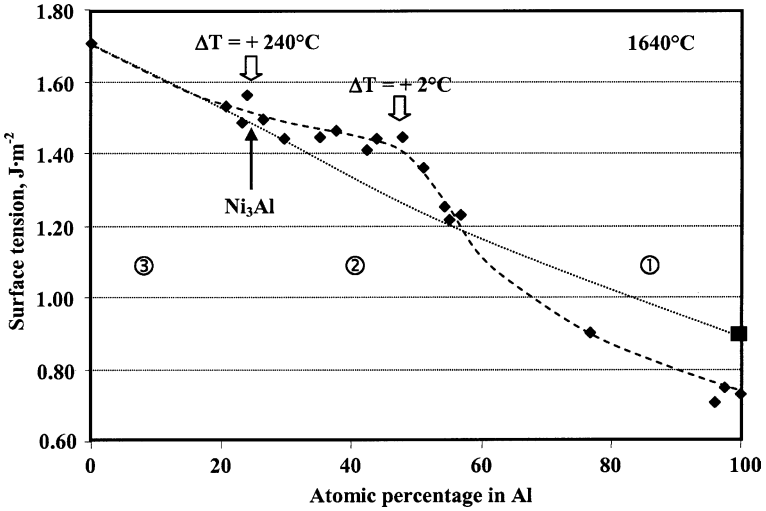

Fig. 7. Experimental results obtained by Eremenko et al. [21] on the Ni–Al system. The curve is the classical interpretation of these experimental results leading to a plateau near 40 at% Al. ΔT is the difference between the experimental isotherm and the liquidus temperature. The square represents an estimation of the surface tension for pure aluminum at 1640°C.

Co (9.3), Cr (7.6), Al (12.6), Ta (2.2), Re (1.0), W (2.0), Ti (1.3), and Mo (0.4) [13]. Energy dispersive X-ray (EDX) analyses have been mainly performed on the samples processed by the drop-weight method. A first remarkable result is that surface and bulk compositions are found to be the same at the level of both the dropping tip and the collected droplet. Excellent agreement between bulk and initial (solid part) compositions is obtained for all elements, including Al and refractory metals. Microsegregation in the directionally solidified dendritic-cellular structure of CMSX-4® superalloy has been studied by Ma and Grafe [21]. Comparison of segregation distributions across the cell shows that both amounts of Al and Ta tend to increase significantly toward the cell surface (with a subsequent enrichment of the interdendritic region compared to the dendrite core) while Re and W show the opposite behavior. These trends are confirmed, when comparing the compositions derived for the dendrites, interdendritic regions, and surfaces. So, the higher content of Al at the surface (+20%) may also partly result from the solidification process, in addition to a segregation effect in the liquid state.

In order to gain some more insight into the behaviour of the multicomponent alloy CMSX-4®, it is helpful to compare it to its reference

binary alloy system, Ni–Al, and in particular to the Ni_3Al intermetallic compound, which forms by peritectic reaction at 1395°C. Surface tension measurements have already been performed on Ni–Al alloys, especially by Eremenko et al. [22]. The variation of the surface tension against the aluminum composition has been established for isotherms at 1640°C (Fig. 7), leading to the identification of three domains. Starting from pure Al, the first domain is dominated by the classical controversy on the surface tension value for pure aluminum. As a matter of fact, a value of $1.05\,J{\cdot}m^{-2}$ has been recently reported by Sarou-Kanian et al. [23] for oxygen-free liquid aluminum, in agreement with other scarce measurements, while a more widely accepted value (even though probably biased by oxygen contamination) is $0.87\,J{\cdot}m^{-2}$ [2]. The second part corresponds to a plateau that has been attributed to compound formation in the melt. However, this conclusion should be carefully re-examined, since the difference between the isotherm and the liquidus temperature becomes very small, passing through a minimum of 2°C at 50 at% Al. Considering the scatter of the experimental data, the presence of a plateau is disputable. An assessment of compound formation in the liquid state should be based from neutron diffraction studies performed on highly stable levitated droplets [24]. The third domain corresponds to the most robust experimental part, and extends to the Ni_3Al compound; a value of $1.49\,J{\cdot}m^{-2}$ at 25 at% Al can be derived from a best fit of experimental results. Moreover, a temperature coefficient of $0.16 \times 10^{-3}\ J{\cdot}m^{-2}{\cdot}K^{-1}$ can also be obtained from experiments reported in a quite equivalent composition range (see Fig. 4 in Ref. [25]), leading to a reference value of $1.53\,J{\cdot}m^{-2}$ at 1380°C.

In order to assess the physical consistency of our measurements, we have estimated surface- tension values for CMSX-4® and Ni_3Al alloys from a linear addition of the pure substances' σ^m values based on atomic percentages (nominal composition). In the case of the Ni_3Al alloy, we obtain $1.56\,J{\cdot}m^{-2}$ or $1.61\,J{\cdot}m^{-2}$, depending on the choice for aluminum. If we apply the same procedure to CMSX-4®, we obtain $1.67\,J{\cdot}m^{-2}$ or $1.69\,J{\cdot}m^{-2}$. To sum things up, the following sequences [experimental value/"low" calculation/"high" calculation] are obtained, namely $[1.49/1.56/1.61]\,J{\cdot}m^{-2}$ for Ni_3Al and $[1.59/1.61/1.69]\,J{\cdot}m^{-2}$ for CMSX-4®. In the same way the ratios σ (Ni_3Al)/σ (CMSX-4®) are [0.94/0.97/0.95]. The calculation for the measured CMSX-4® surface composition leads to a negligible lowering of the surface tension ($-0.02\,J{\cdot}m^{-2}$) compared to that derived from the measured bulk composition. So, the experimental increase of the surface tension from Ni_3Al to CMSX-4® is of the same order of the effect that can be deduced by applying the straightforward calculation of the surface tension.

6. CONCLUSION

The surface tension of the CMSX-4® superalloy has been determined by both the drop-weight and oscillating-drop methods with a difference in measurements at the liquidus temperature which is smaller than the combined uncertainties of the methods. Assuming that the drop-weight method should lead to a reference value at the melting temperature, this study also demonstrates that the Cummings and Blackburn relation can be used for accurate measurements of the surface tension of complex alloys by the oscillating-drop method. By reference to Eremenko's work [22], the small experimental increase of the surface tension between the Ni_3Al alloy and the CMSX-4® superalloy is of the order of the effect deduced by applying a straightforward estimation of the surface tension derived from a linear addition of the pure substances' values (atomic percentages). Moreover, the temperature coefficient appears to be quite similar for the two materials. More generally, the application of the straightforward calculation used here leads one to expect a very narrow spread of the surface tension for Ni-base superalloys. Considering the compositions given in Ref. [13], almost the same surface tension can be derived for a set of 16 superalloys, including first generation single-crystal superalloys and Re-containing single-crystal alloys. Indeed, the variation from 1.68 to $1.72\,J{\cdot}m^{-2}$ ($\Delta\sigma/\sigma \approx 1\%$) indicates that our measurements, for this particular thermophysical property, should be characteristic of this class of materials.

Thus, this study is encouraging for the application of the drop-weight and oscillating-drop methods to complex industrial alloys. Nonetheless, a thorough interpretation of surface-tension measurements on complex alloys requires some insights from the solidification process due to the occurrence of strong microsegregation effects. The study of model alloys could thus be very helpful, as already demonstrated by Rüsing et al. [26] when considering the quaternary Ni–Al–Ta–Re system to investigate the Re distribution. Finally, this study clearly shows that considerable work on surface-tension measurements on basic binary or ternary systems remains to be done. The possibility to obtain the value for oxygen-free liquid aluminum by containerless processing obviously provides a new perspective for a new look at the Ni–Al system.

ACKNOWLEDGMENTS

Both DLR and CEA contributions have been realized in the framework of the ESA-Thermolab project "High-Precision Thermophysical Property Data of Liquid Metals for Modelling of Industrial Solidification

Processes", coordinated by H.J. Fecht (University of Ulm). Financial support is gratefully acknowledged. The CMSX-4® superalloy has been obtained by courtesy of Doncasters in the course of this project. Many thanks to the entire ThermoLab team for exciting discussions. Support from CNES within the frame of the now defunct GRAMME agreement between CNES and CEA is also gratefully acknowledged.

REFERENCES

1. N. Eustathopoulos, M. G. Nicholas, and B. Drevet, *Wettability at High Temperature*, Vol. 3 (Pergamon Materials Series, Amsterdam, 1999).
2. B. J. Keene, *Int. Mat. Rev*. **38**:157 (1993).
3. I. Egry, G. Lohöfer, I. Seyhan, S. Schneider, and B. Feuerbacher, *Int. J. Thermophys*. **20**:1005 (1999).
4. I. Egry, S. Sauerland, and G. Jacobs, *High Temp. – High Press*. **26**:217 (1994).
5. P. F. Paradis, T. Ishikawa, and S. Yoda, *Int. J. Thermophys*. **23**:825 (2002).
6. G. Wille, F. Millot, and J. C. Rifflet, *Int. J. Thermophys*. **23**:1197 (2002).
7. See for a review, B. Vinet, *Int. J. Mater. Product Technol*. **20**:392 (2004).
8. S. Schneider, I. Egry, and I. Seyhan, *Int. J. Thermophys*. **23**:1241 (2002).
9. B. Vinet, J. P. Garandet, and L. Cortella, *J. Appl. Phys*. **73**:3830 (1993).
10. B. Vinet and J. P. Garandet, *Proc. 2nd Int. Conf. High Temp. Capillarity*, N. Eustathopoulos, ed. (Reproprint Bratislava, 1995), pp. 223–227.
11. J. P. Garandet, B. Vinet, and P. Gros, *J. Coll. Int. Sci*. **165**:351 (1994).
12. B. Vinet, B. Marie, J. P. Garandet, L. Domergue, and B. Drevet, *Int. J. Thermophys*. **25**:245 (2004).
13. R. W. Broomfield, D. A. Ford, H. K. Bhangu, M. C. Thomas, D. J. Frasier, P. S. Burkholder, K. Harris, G. L. Erickson, and J. B. Wahl, in *Rhenium and Rhenium Alloys*, B. D. Bryskin, ed. (The Mineral, Metals & Materials Society, Warrendale, Pennsylvania, 1997), pp. 731–754.
14. W. Harkins and F. E. Brown, *J. Am. Chem. Soc*. **41**:499 (1919).
15. Lord Rayleigh, *Proc. R. Soc*. **29**:71 (1879).
16. D. Cummings and D. Blackburn, *J. Fluid Mech*. **224**:395 (1991).
17. F. H. Busse, *J. Fluid Mech*. **142**:1 (1984).
18. S. Sauerland, K. Eckler, and I. Egry, *J. Mater. Sci. Lett*. **11**:330 (1992).
19. Determined in the course of the Thermolab Project by University of Turin, NPL, and University of Ulm.
20. S. F. Chen and R. A. Overfelt, *Int. J. Thermophys*. **19**:817 (1998).
21. D. Ma and U. Grafe, *Mater. Sci. Eng. A* **270**:339 (1999).
22. V. I. Eremenko, V. I. Nizhenko, and Yu. V. Naidich, *Izv. Akad. Nauk SSSR Metallurgiya i Topivo*. **3**:150 (1961).
23. V. Sarou-Kanian, F. Millot, and J. C. Rifflet, *Int. J. Thermophys*. **24**:277 (2003).
24. D. Holland-Moritz, G. Jacobs, and I. Egry, *Mater. Sci. Eng. A* **294**:369 (2000).
25. G. D. Ayushina, E. S. Levin, and P. V. Gel'd, *Russ. J. Phys. Chem*. **43**:1548 (1969).
26. J. Rüsing, N. Wanderka, U. Czubayko, V. Naundorf, D. Mukherji, and J. Rösler, *Scripta Materialia* **46**:235 (2002).